LONGITUDINAL WAKEFIELDS AND IMPEDANCE IN THE CSNS/RCS*

N. Wang[#], Q. Qin

Institute of High Energy Physics, Beijing 100049, P.R.China

Abstract

With the more general expressions developed for the wakefield generated by non-ultrarelativistic beam [1], the impedances of some main vacuum parts of the Rapid Cycling Synchrotron (RCS) of China Spallation Neutron Source (CSNS) are calculated and compared with the relativistic case. An impedance model is then proposed for the whole ring. With this impedance model, beam instabilities in the CSNS/RCS are investigated.

INTRODUCTION

The RCS ring of CSNS will work at the injection energy of 80 MeV and extraction energy of 1.6 GeV [2]. In this energy region, the beam velocity is significantly different from the speed of light c, and consequently the wakefield generated by beam is quite different from that in the ultrarelativistic limit [3].

In this paper, the longitudinal impedance of some main vacuum parts of the RCS ring is evaluated at the injection and extraction energy. The beam aperture used in the calculation is shown in Fig. 1.
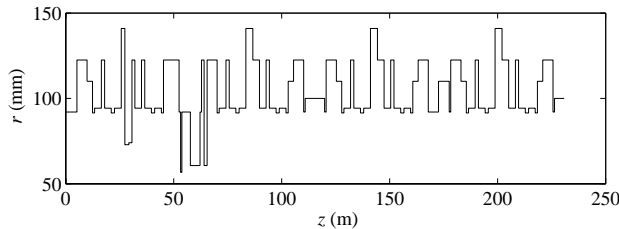

Figure 1: Schematic layout of the beam pipe aperture.

IMPEDANCE MODEL

Generally, a point charge q moving on the axis of the beam pipe with a velocity βc is considered. The current density in the time region can be expressed with the δ function

$$\vec{j} = \frac{q\beta c}{2\pi r}\delta(r)\delta(z-\beta ct)\vec{e}_z \cdot \qquad (1)$$

The impedances are all evaluated analytically at the radial position of $r = 0$. As the low frequency impedance has the dominant effect on the proton beam, here we evaluate the impedance in the range of 0~100MHz. In the following, we first give the numerical results of some main origin of impedance, and then the impedance model with independent variable ω is derived by fitting.

Resistive Wall

The resistive wall impedance in the RCS ring mainly

comes from the stainless steel chambers. The numerical results contributed by the stainless steel chambers in the whole ring are got according to the Eq. (57) in Ref. [3], which gives a good approximation at low frequency. Then by fitting the frequency map of the impedance, we obtain the expressions of impedance as a function of frequency

$$Z_{//,rev}^{inj} = 0.01 \cdot (\mathrm{sgn}(\omega) + j)\sqrt{\omega}\left(59.17 - 2.00\times10^{-5}\omega^2\right),$$

$$Z_{//,rev}^{ext} = 0.01 \cdot (\mathrm{sgn}(\omega) + j)\sqrt{\omega}\left(59.17 - 5.55\times10^{-7}\omega^2\right), (2)$$

where ω is the angular frequency in unit of MHz.

Ceramic Chamber

Ceramic chambers will be used in the magnetic regions to avoid shielding of fast changing magnetic field by metallic chambers and to suppress the heating from eddy current. In order to reduce the impedance, stripes made from copper will be added in the outer surface. The inner surface of the chamber will be coated with TiN to suppress the secondary electron emission.

In order to get the analytical result, we replace the stripes to a conducting beam pipe. Impedance of multi-layer beam pipe has been derived in Ref. [1] by using field matching method. By eliminating the space charge impedance from Eq. (62) in Ref. [1], the resistive wall impedance at a radial position r can be evaluated by

$$Z_{//,rev} = -\frac{jZ_0 c k_r}{2\pi\omega a_1}\left[\frac{\kappa M I_0(k_r r)}{I_0(k_r a_1)\left(\kappa M I_1(k_r a_1) + I_0(k_r a_1)\right)}\right], (3)$$

where $Z_0 = 377\Omega$ is the free space impedance, $k_r = \omega/\beta\gamma c$, γ is the relativistic energy, a_1 is the inner aperture of the chamber, I_0 and I_1 are modified Bessel functions and κ, M are expressions defined in Ref. [1].
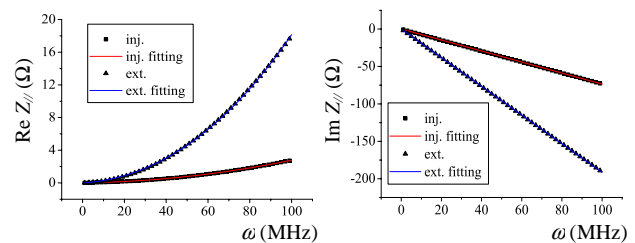

Figure 2: Longitudinal impedance of ceramic chambers in the RCS ring for both injection and extraction energy.

The real and imaginary parts of the longitudinal impedance of the ceramic chamber are shown in Fig. 2. The square and triangle symbols denote the impedance at injection and extraction energy, respectively, and the corresponding solid lines are results of fitting. The difference between the impedance at injection and extraction energy is clear. The impedance of the ceramic chambers obtained by fitting can be expressed as

$$Z_{//}^{inj} = 0.0016\sqrt{\omega}\left(\omega + 0.0070\omega^2\right) + j0.73\omega,$$

05 Beam Dynamics and Electromagnetic Fields

D04 Instabilities - Processes, Impedances, Countermeasures

$$Z_{//}^{ext} = 0.0080\sqrt{\omega}\left(\omega+0.013\omega^2\right)+ j1.92\omega. \quad (4)$$

Step

Wakefield of a step with semi-infinite long side tubes for velocity $v<c$ has been derived by Kheifets and Heifets in Ref. [4], in which two different cases of step-in and step-out are considered. The geometry is shown in Fig. 3.
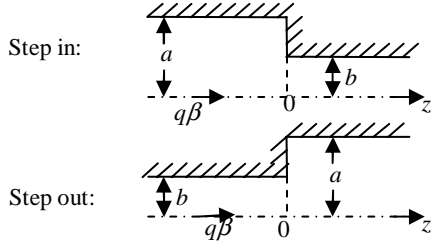

Figure 3: Geometry of step-in and step-out structures

In the nonrelativistic case, the longitudinal coupling impedance for the step-in structure at radial position r is

$$Z_{in}(k) = \frac{2\pi i}{q}\left[\sum_m B_m^+ J_0(v_m r/b)\frac{k_0^2-\lambda_{bm}^2}{k-\lambda_{bm}} , \\ -\sum_n B_n^- J_0(v_n r/a)\frac{k_0^2-\lambda_{an}^2}{k+\lambda_{an}}\right] \quad (5)$$

with

$$\begin{cases} B_m^+ = d_m + \sum_n f_{mn}B_n^-, \\ B_l^- \lambda_{al}J_l^2(v_l) = D_l - \sum_n \frac{\lambda_{bn}v_n^2 J_1^2(v_n)}{v_l^2}f_{nl}B_n^+, \end{cases}$$

and for the step-out one, the longitudinal impedance is

$$Z_{out}(k) = -\frac{2\pi i}{q}\left[\sum_m B_m^- J_0(v_m r/b)\frac{k_0^2-\lambda_{bm}^2}{k+\lambda_{bm}} , \\ -\sum_n B_n^+ J_0(v_n r/a)\frac{k_0^2-\lambda_{an}^2}{k-\lambda_{an}}\right] \quad (6)$$

with

$$\begin{cases} B_m^- = d_m + \sum_n f_{mn}B_n^+, \\ B_l^+ \lambda_{al}J_l^2(v_l) = -D_l - \sum_n \frac{\lambda_{bn}v_n^2 J_1^2(v_n)}{v_l^2}f_{nl}B_n^-. \end{cases}$$

Here, $k_0=\omega/c$, $k=\omega/\beta c$, and other variables in the above expressions have the same meaning as those in Ref. [4].
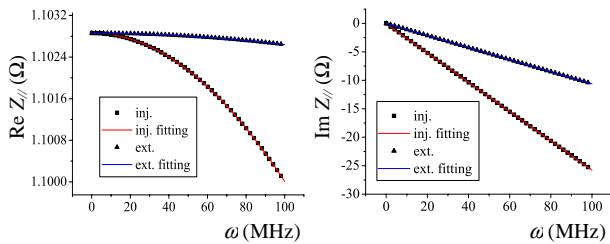

Figure 4: Longitudinal impedance of steps in the RCS ring for both injection and extraction energy.

The longitudinal impedance for the steps is shown in Fig 4. The difference is distinct for different beam energy. Fitting the two curves in Fig. 4 we can obtain the corresponding longitudinal impedance models of steps

$$Z_{//}^{inj} = 1.10 - 2.85\cdot10^{-7}\omega^2 + j(0.026+0.26\omega),$$
$$Z_{//}^{ext} = 1.10 - 2.20\cdot10^{-8}\omega^2 + j(0.000090+0.11\omega). \quad (7)$$

Kicker

The extraction system consists of 10 kickers, which are important contributions to the longitudinal coupling impedance for the RCS ring.

Longitudinal impedance of some simplified kicker models in the ultrarelativistic limit has been given in Ref. [5]. Here, we use the simplified model 2 in Ref. [5] stretched in Fig. 5, which has been proved to make a good agreement with measurement.
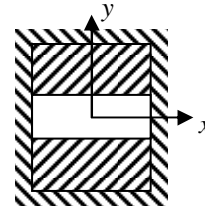

Figure 5: Simplified kicker model

We extend the results to the general case of $v < c$, and the longitudinal impedance can be expressed as

$$\frac{Z_{//}}{L} = -\sum_n \frac{A_n}{B_n}, \quad (8)$$

with

$$A_n = -M\exp(jk_{2n}b)\big[k_{2n}\cos(x_1)\big(jk_{2n}(k^2-k_0^2\varepsilon_r\mu_r) \\ -k^2 k_{3n}\varepsilon_r\cot(x_2)/\gamma^2\big)+\sin(x_1)\big(k^2(k_r^2\varepsilon_r\mu_r/\gamma^2 \\ -k_{1n}^2\beta^2+k_{1n}^2\varepsilon_r\mu_r)+jk_{2n}k_{3n}k_r^2\mu_r\tan(x_2)\big)\big]$$

$$B_n = kk_{2n}\big[-k_{2n}k_{3n}\varepsilon_r\cos(x_1)^2\cot(x_2) \\ +\big(k^2+(-k_0^2+k_r^2)\varepsilon_r\mu_r+k_{1n}^2(1+\varepsilon_r\mu_r)\big), \\ \cos(x_1)\sin(x_1)-k_{2n}k_{3n}\mu_r\sin(x_1)^2\tan(x_2)\big]$$

$$M = \lim_{b\to0}\frac{Z_0 k_r}{2\pi a\beta}\int_{-a}^a dx \sum_{m=-\infty}^\infty E_y^m \cos(k_{1n}x),$$

$$E_y^m = (-1)^m \frac{b}{\sqrt{(x-2ma)^2+b^2}}K_1\left(k_r\sqrt{(x-2ma)^2+b^2}\right),$$

$$k_{1n} = (2n+1)\pi/2a, n=0,1,2,...,$$

$$k_{1n}^2+k_{2n}^2 = -k_r^2,\ k_{1n}^2+k_{3n}^2 = k_0^2\mu_r\varepsilon_r-k^2,$$

$$x_1 = k_{2n}b, x_2 = k_{3n}(b-d).$$

The longitudinal impedance of the kickers is shown in Fig. 6. The corresponding impedance models are

$$Z_{//}^{inj} = \frac{306.35}{(1+1.07\times10^4\omega^{-2})^2} - \frac{j169.97}{1-0.0092\omega-135.49\omega^{-1}},$$

$$Z_{//}^{ext} = \frac{55.43}{(1+1.08\times10^4\omega^{-2})^2} - \frac{j92.89}{1-0.0090\omega-225.65\omega^{-1}}. \quad (9)$$
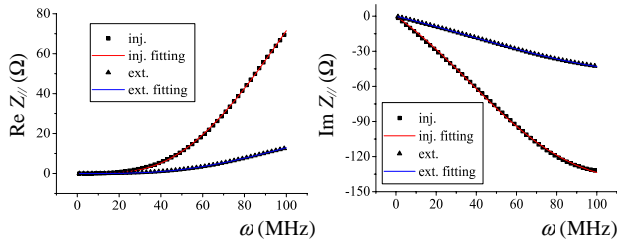
Figure 6: Longitudinal impedance of extraction kickers in the RCS ring for both injection and extraction energy.

Bellows

Bellows will be used in the arc of the RCS to connect different chambers. The corrugations with a period of 16mm and a depth of 18 mm are considered. The bellows chambers have a pipe aperture of 141 mm and a total length of 11.76 m.

Here, we use the conclusions given in Ref. [6] that the impedance of each corrugation is independent of its number, and the impedance of a corrugation is estimated based on the result given in Ref. [7]. The final result is obtained by multiplying them the number of corrugations.
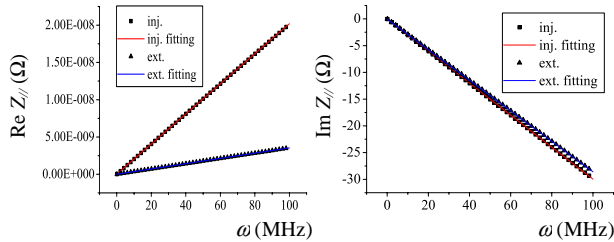

Figure 7: Longitudinal impedance of bellows in the RCS ring for both injection and extraction energy.

The numerical results are shown in Fig. 7, and the fitted impedances are

$$Z_{//}^{inj} = j0.30\omega,$$
$$Z_{//}^{ext} = j0.29\omega. \qquad (10)$$

Comparison with Relativistic Model

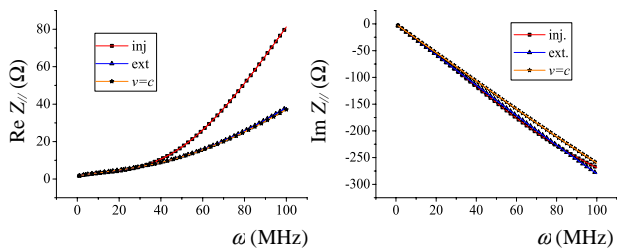Up to now, we have obtained the impedance model for the main vacuum parts of the RCS ring.

Figure 8: Comparison of the non-ultrarelativistic and ultrarelativistic impedance model.

The result is presented and compared with the relativistic case in Fig. 8, in which the curves with square makers correspond to injection energy, the curves with

triangles correspond to extraction energy, and the curves with stars correspond to the ultrarelativistic case. From the results, we can find that the nonrelativistic correction could be considered in evaluating the impedance of low energy beams for the low frequency impedance when the machine is in big or medium size. But for a small size synchrotron, the nonrelativistic correction should be taken into account.

INSTABILITY

The instability is estimated by using the Keil-Schnell criterion [9]

$$\left|\frac{Z_{//}}{n}\right| < \frac{|\eta|E_0}{eI_0\beta^2}\left(\frac{\Delta E}{E_0}\right)^2_{FWHM}, \qquad (11)$$

and we get $|Z_{//}^{in}/n| < 892\Omega$, $|Z_{//}^{out}/n| < 809\Omega$.

According to the longitudinal impedance estimation above, in addition to the space charge impedance [8], the longitudinal microwave instability should not happen. But other instabilities, especially the transverse ones and the electron cloud effect, more analyses are under way.

SUMMARY

The nonrelativistic longitudinal impedance model has been derived for some main vacuum parts in the RCS ring. The result is compared with the relativistic limit, which demonstrates that the nonrelativistic correction should be considered in evaluating the impedance of low energy proton beam, especially for the small synchrotrons.

The impedance shows no longitudinal instabilities will be happen. But much work needs to do on the particle tracking simulation for instabilities.

The transverse impedance derivation in the case of $v<c$ is under going, and the corresponding instability will be analyzed subsequently.

ACKNOWLEDGEMENT

REFERENCES

[1] N. Wang and Q. Qin, Phys. Rev. ST Accel. Beams 10, 111003 (2007).
[2] J. Wei, et al, Proc. Of EPAC'06, June 2006.
[3] F. Zimmermann and K. Oide, Phys. Rev. ST Accel. Beams 7, 044201 (2004).
[4] S. A. Kheifets and S. A. Heifets, SLAC-PUB-3965 (1986).
[5] H. Tsutsui, CERN-SL-2000-004 AP (2000).
[6] King-Yuen Ng, Proc. Of PAC'87, p1051 (1987).
[7] H. Henke, CERN-LEP-RF/85-41.
[8] N. Wang and Q. Qin, Proc. Of APAC'07, Jan. 2007.
[9] E. Keil and W. Schnell, CERN Report TH-RF/69-48 (1969)

05 Beam Dynamics and Electromagnetic Fields

D04 Instabilities - Processes, Impedances, Countermeasures